On the Applicability of Resonance Forms in Pyrimidinic Bases. II. QTAIM Interpretation of the Sequence of Protonation Affinities

María J. González Moa[†,‡] and Ricardo A. Mosquera*[,‡]

Departamento Química Orgánica and Departamento Química Física, Universidade de Vigo, Lagoas-Marcosende, 36200-Vigo, Galicia, Spain

Received: December 1, 2004; In Final Form: March 2, 2005

The atomic properties of neutral and protonated forms of uracil and some model compounds, computed from B3LYP/6-31++G**//B3LYP/6-31G** charge densities with the QTAIM theory, indicate that σ electron reorganization plays a significant role in the protonation processes. This reorganization is substantially different for O=C−C=C and O=C−C−X (X = N, O) units, involving transfers of electron population between all atoms in the first case but not across the C−X bond in the second unit. O-Protonation is basically favored over the N-protonation because of the lower electron population transferred to the proton. The stability sequence of N-protonated forms can be rationalized in terms of the closer position of the proton, when attached to N3, to regions of larger electron population (carbonyl groups).

Introduction

In a recent paper,[1] using the Quantum Theory of Atoms in Molecules (QTAIM),[2,3] we have demonstrated that neither the evolution experienced by the atomic properties of uracil and cytosine upon protonation nor the delocalization indexes calculated for the neutral species can be explained by the resonance model (RM).[3] Similar conclusions were also obtained for other heterocycles containing π delocalized systems,[4] using both QTAIM theory and stockholder charges[5,6] (based on the Hirshfeld scheme[7]). Other previous evidence about the shortcomings of the RM were also published[8−13] as was detailed in Part I of this paper.[1]

According to the RM, the protonations of uracil at O10 (Figure 1) are predicted to be more stable than those at O8 because four resonance forms can be drawn for the first one, whereas only three correspond to the protonations at O8 (Figure 2). This prediction keeps in line with the calculated proton affinities (PAs)[1] shown in Table 1. Nevertheless, if the electron charge reorganization in the process is not described correctly by the RM, it is not reasonable to accept the RM explanation for the sequence of relative stabilization of protonated forms of these molecules. Therefore, looking for a more reliable interpretation, we have analyzed how the population, $N(\Omega)$, and the energy, $E(\Omega)$, of every atom, Ω, evolve in the diverse protonation processes. It is our goal to answer the following questions: (a) why is the protonation of uracil more favored at O10 than at O8? and (b) why is the protonation of uracil at N3 preferred to that at N1? These questions are answered in different epigraphs of this paper.

Computational Details

B3LYP/6-31G** full optimizations were carried out for the neutral and protonated forms of uracil and some model molecules (vinyl ketone, formamide, *N*-methylformamide, methyl formiate, and formaldehyde) using the Gaussian98 program.[14]

* Corresponding author. E-mail: mosquera@uvigo.es.
† Dpto. Química Orgánica.
‡ Dpto. Química Física.

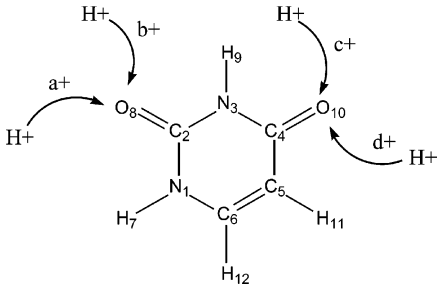

Figure 1. Atom numbering for uracil and nomenclature for its possible O-protonations.

All the optimized structures were characterized as minima in the frequency calculation. The QTAIM atomic properties were calculated using the AIMPAC[15] program on charge densities calculated at the B3LYP/6-31++G** level and performing a σ/π separation of the atomic electron populations.

We observed that the error in the determination of the interatomic surfaces of the carbonyl carbons, measured by $L(\Omega)$,[2] was substantially reduced when the integrations were performed considering the existence of second and third intersections between every integration ray and those interatomic surfaces. Thus, the absolute values achieved for $L(\Omega)$ were always smaller than 4.6 10^{-3} au. Integration errors expressed as differences between total properties and those obtained by summation of properties of the fragments [N-$\Sigma N(\Omega)$ or E-$\Sigma E(\Omega)$] were always smaller (in absolute value) than 3.6 10^{-3} au and 2.7 kJ mol^{-1}, respectively, which was found to be accurate enough as compared with other works carried out at similar theoretical levels.

Results and Discussion

O-Protonation of Uracil. According to the RM, the positive charge of the proton should be delocalized over more atoms when it is bonded to O10 than when attached to O8 (Figure 2). This would explain why protonations at O10 are preferred to those at O8 in a range from 27.9 to 44.7 kJ mol^{-1} (as computed at the B3LYP/6-31++G**//B3LYP/6-31G** level;[1] Table 1).

10.1021/jp044529k CCC: $30.25
Published on Web 04/02/2005

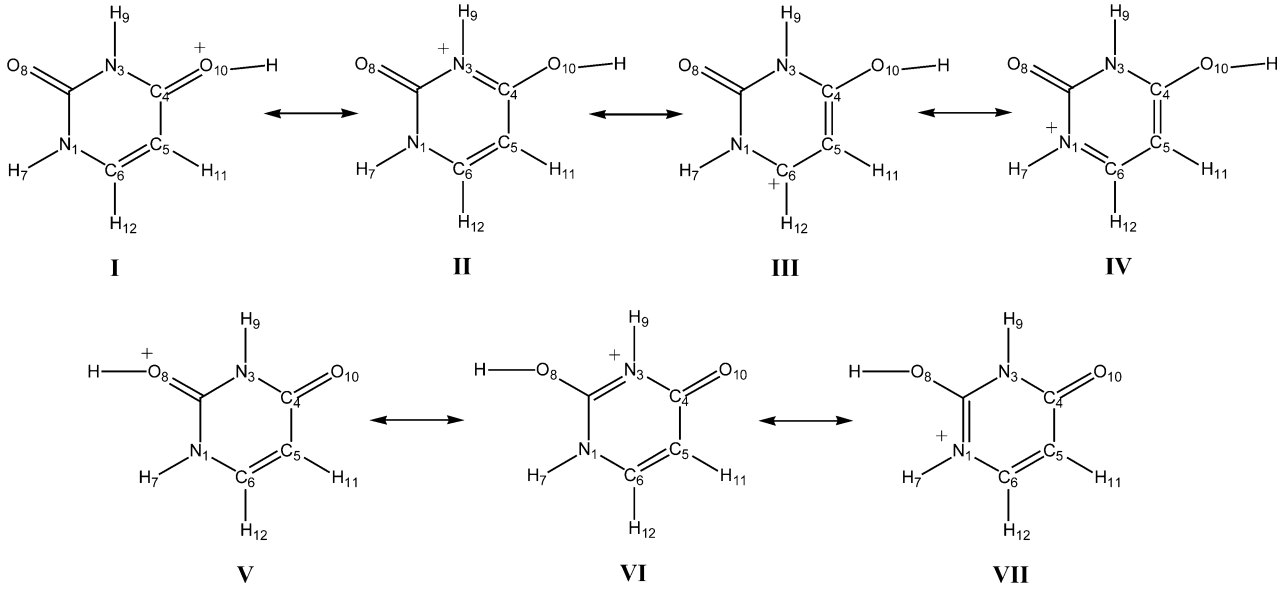

Figure 2. Resonance forms for the uracil protonations at O10 (I−IV) and O8 (V−VII).

TABLE 1: Proton Affinities, PA, and Variation of the Atomic Populations (in au and Multiplied by 10^3) for the Diverse O-Protonations of Uracil (Figure 1)[a]

		$10^3\,\Delta N(\Omega)$ [au]									
molecule	PA [kJ mol^{-1}]	**N1**	**N3**	**C6**	**ΣH**	**C5**	**O8**	**O10**	**C2**	**C4**	$N(H^+)^b$ [au]
a+	**809.1**	**15**	**−10**	**55**	**−222**	**−51**	**−79**	**−73**	**20**	**9**	**0.341**
b+	**814.1**	**18**	**−11**	**31**	**−228**	**−49**	**−76**	**−69**	**20**	**31**	**0.337**
c+	**842.0**	**−13**	**18**	**−109**	**−230**	**−75**	**−70**	**−65**	**10**	**185**	**0.351**
d+	**853.8**	**−15**	**23**	**−129**	**−225**	**−47**	**−73**	**−57**	**1**	**180**	**0.342**

[a] All properties were calculated from B3LYP/6-31++G**//B3LYP/6-31G** charge densities. [b] Atomic electron population in the atomic basin of the proton.

However, contrary to what should be expected according to the RM, the electron population of the nitrogen atoms is not significantly reduced by O-protonation. It even increased in some cases (Table 1). On the contrary, the atomic population of C6 displays the trends expected according to the RM, decreasing when O10 is protonated. This fact could indicate that the O=C−C=C and O=C−N−C units have a different behavior during protonation: the former follows a trend that keeps in line with the RM, and the latter does not. To prove this hypothesis, we have computed the QTAIM atomic properties of neutral and O-protonated forms of the s-trans conformer of vinyl ketone, formamide, and *N*-methylformamide.

Two already described facts are corroborated by the results obtained for the O-protonation of uracil and those obtained for the remaining models employed in this work (formaldehyde, formamide, *N*-methylformamide, and methyl formiate). Thus, (i) the proton keeps a very important positive charge (between 0.70 and 0.65 au), which makes the protonated form closer to a $R-O-H^+$ structure than to a $R-O^+-H$ one, as was previously observed for other carbonyl compounds[1,16] and ethers;[11−13] and (ii) practically all of the electron population gained by the proton is σ (π transfers do never reach 0.01 au in the series) as was also previously reported using the σ/π separation within QTAIM[1,4] and stockholder[4] frameworks. Regarding the first point, the substantial positive charge at the proton, we noticed that the usual criticisms on the magnitude of QTAIM charges[17−19] have been recently refuted by Bader and Matta in a recent issue of this journal.[20]

Looking at the variations of the atomic π-electron populations, $N^{\pi}(\Omega)$, with some detail, we observe that more than 85% of the total change experienced by the π atomic populations of vinyl ketone in its O-protonation are localized at C3 and O4

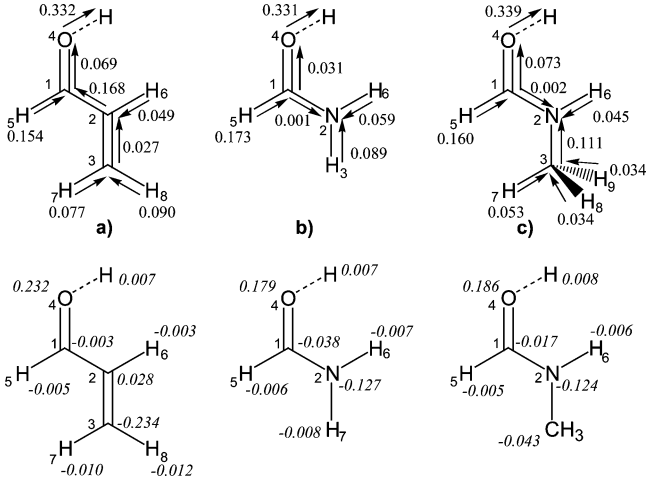

Figure 3. B3LYP/6-31++G**//B3LYP/6-31G** QTAIM computed σ electron interatomic transfers (values on continuous arrows) and variation of atomic π electron populations (values in italics) for (a) vinyl ketone, (b) formamide, and (c) *N*-methylformamide. All values are in au. Interatomic transfers were computed assuming that the whole variation of the atomic population, $\Delta N(\Omega)$, of a terminal atom is due to the electron transfer with its neighbor. $\Delta N(\Omega)$ for the remaining atoms is obtained by adding the transfers to all the atoms they are attached.

(Figure 3), with a transfer of 0.23 au from C3 to O4. This transfer takes place as a continuous variation of the π-electron molecular density (Figure 4), which reinforces the π-electron density at the C1−C2 bond region and depletes those at C2=C3 and C1=O4 (just as the RM suggests). O-Protonation of formamide and *N*-methylformamide increases N^{π}(O4) (in 0.179 and 0.186 au, respectively). This charge is mainly taken from

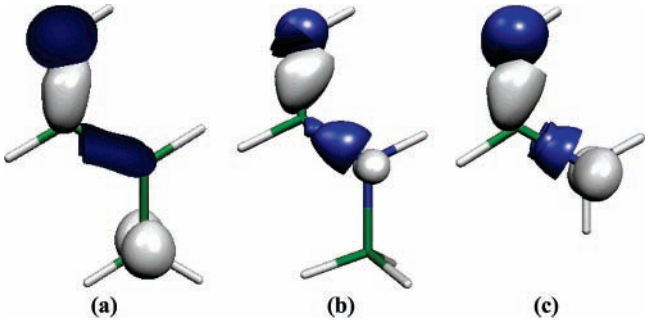

Figure 4. Plots for the variation of the molecular π-electron density experienced in the O-protonations of vinyl ketone (a), *N*-methylformamide (b), and formamide (c). Zones in blue correspond to reinforcements and zones in gray to depletions in the protonated forms. Plots done with MOLEKEL program.[21,22]

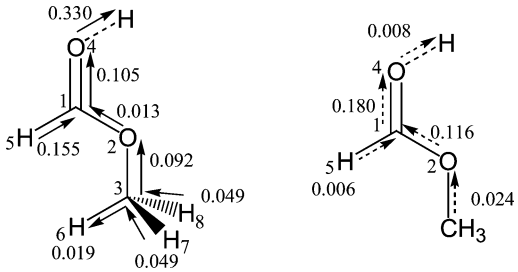

Figure 5. B3LYP/6-31++G**//B3LYP/6-31G** QTAIM computed σ (continuous arrows) and π (points arrow) electron interatomic transfers for methyl formiate. All values are in au.

N^{π}(N2) (depleted 0.127 au in formamide and 0.124 au in *N*-methylformamide, Figure 3, which represents 68 and 64%, respectively, of the total modification of atomic π populations). These modifications take place increasing the π-charge density at C−N and depleting it at the C═O bond (Figure 4), which is again in line with the RM prediction.

We observe that the changes in the π electron atomic populations due to protonation are accompanied by intense reorganization of the σ-electron density in the three molecules (Figure 3) that are not considered by the RM. The modification experienced by each atom depends on various factors that are commented on here for the protonation of vinyl ketone: (a) the atomic number of the attractor; thus, H7 and H8 provide more electron charge than C3 despite being further away from the proton; (b) distance to the proton (thus, ΔN^{σ}(H5) > ΔN^{σ}(H8) > ΔN^{σ}(H7)); (c) bond orientation: the transfer or electron charge further from the proton explains the small amount of σ charge transferred from H6 to C2; and (d) the balance between σ and π transfers; thus, the substantial amount of π electron population received by the oxygen causes C1 (closer to the proton than C2) to lose less σ electron population than C2.

The reorganization of the σ-electron population is also intense in formamide and *N*-methylformamide (Figure 3), but there is a significant different trend: there is practically no σ-charge transfer between the NR_2 and the $HCOH^+$ units.

The same behavior is observed when the conjugated C−N bond of *N*-methylformamide is replaced by a C−O bond (methyl formiate, Figure 5); there is an important π-charge transfer from O2 and C1 (0.092 and 0.058 au, respectively, amounting to 51 and 32% of the total π modifications) to O4 (that receives 0.172 au, 95.5% of the total π charge transferred), which is exceeded by the variations experienced by the atomic σ-electron populations. These variations take place minimizing the transfer of the σ-charge from the other heteroatom (N in formamide and *N*-methylformamide and O in methyl formiate) to the C═O bond (−0.001, −0.002, and 0.013 au for, respectively, formamide, *N*-methylformamide, and methyl formiate).

TABLE 2: Differences between the Changes in the Atomic Electron Population Due to Protonations d+ and a+ of Uracil, $\Delta\Delta N(\Omega)=\Delta N^{d+}(\Omega)-\Delta N^{a+}(\Omega)$, and Energy, $\Delta\Delta E(\Omega)$[a]

atom	$10^3\,\Delta\Delta N(\Omega)$ [au]	$\Delta\Delta E(\Omega)$ [kJ mol^{-1}]	$10^3\,\Delta\Delta N^{\sigma}(\Omega)$ [au]	$10^3\,\Delta\Delta N^{\pi}(\Omega)$ [au]
H^+	1	−4.4	1	0
Oα	23	−45.4	−9	33
Cβ	163	−282.4	126	37
O[b]	−2	11.2	0	−1
C[b]	−10	10.7	−11	2
N1	−28	7.2	22	−51
N3	34	−69.2	14	20
C5	5	41.1	−112	117
C6	−186	268.4	−30	−156
H7	−19	31.1	−17	−2
H9	−1	−0.4	−1	0
H11	29	−29.8	23	6
H12	−11	10.4	−7	−4

[a] All properties were calculated from B3LYP/6-31++G**//B3LYP/6-31G** charge densities. [b] Atoms of the unprotonated carbonyl group.

So, we can state that the electron charge gained by the proton during an O-protonation is basically σ and taken from the attached oxygen. At the same time, the oxygen compensates the charge loss receiving σ and π transfers from the rest of the molecule. The presence of another electronegative atom (N or O) in the molecule acts as a barrier to the σ-electron transfer from the rest of the molecule, giving rise to qualitatively different σ-charge reorganizations for the O-protonation of the O═C−C═C and O═C−X (X = OR, NR_2) units. The former involves electronic transfers along the whole molecule, so they are more effective (reduce more the total energy). In contrast, the latter reorganizes almost independently the σ-population of the H_2CO^+ and X units originating higher molecular energies.

Thus, the models here employed allow us to assign the preference for the O10 protonated forms to its simultaneous inclusion in the O═C−C═C and O═C−N−C units, whereas O8 (the least preferred oxygen for protonation) is involved in two O═C−N−C units. The protonation of the O═C−C═C unit gives rise to more extended σ-charge transfers and more intense π reorganizations. This is quantitatively shown in Table 2 using the quantities $\Delta\Delta N(\Omega)$, representing the difference between the electron population experienced by a certain Ω atom in protonations d+ and a+ (Figure 1), and $\Delta\Delta E(\Omega)$, which is the corresponding energy difference. Protonations d+ and a+ have been chosen for generating the most stable cation with the proton bonded, respectively, to O10 and O8 and because they place the proton symmetrically with regard to the N3−H9 bond, which ensures that steric repulsions with this group and the remaining units are similar. We observe that atoms with large $\Delta\Delta N(\Omega)$ values also present significant $\Delta\Delta E(\Omega)$ values, so the relative stabilization of one atom in these protonations is associated to its relative variation of the electron population. The atoms that are affected in a most different way by each protonation are the carbonylic carbon that is β to the proton, C$^{\beta}$, and C6. Thus, protonation d+ differs basically from protonation a+ in the electron charge lost by C6 and in that gained by C$^{\beta}$. This fact agrees with the diverse charge displacements obtained for the O═C−C═C and O═C−NR_2 units in the model molecules (Figure 3). There is also a smaller but significant difference in the stabilization of the oxygen bonded to the proton, $\Delta\Delta E(O^{\alpha})$.

N-Protonation of Uracil. The PAs of these processes were found to be significantly lower (between 67 and 143 kJ mol^{-1}) than those corresponding to the O-protonations.[1] On the other

TABLE 3: Contributions to the Proton Affinity, PA, for the Diverse Protonations of Uracil, Containing the Variations of the Atomic Energy, $\Delta E(\Omega)$, ΔZPVE, and the Difference between Summation of These Contributions and PAs Obtained from Total Molecular Energy, ϵ[a]

	O8 (a+)	O8 (b+)	O10 (c+)	O10 (d+)	N1	N3
ΔE(N1)	−39.5	−107.0	−33.2	−32.3	489.3	−10.9
ΔE(C2)	−101.0	−102.6	13.3	24.6	−52.0	−84.6
ΔE(N3)	−47.7	4.9	−56.1	−116.9	5.8	517.9
ΔE(C4)	14.0	−18.6	−388.4	−383.4	80.5	−238.9
ΔE(C5)	28.7	32.0	81.6	69.8	12.0	88.5
ΔE(C6)	−78.7	−43.3	154.1	189.8	−340.9	43.2
ΔE(H7)	44.9	80.1	75.2	76.0	69.7	71.0
ΔE(O8)	36.5	35.4	−87.0	−83.9	−139.1	−106.2
ΔE(H9)	82.2	53.2	48.2	81.8	78.6	61.3
ΔE(O10)	−95.1	−105.4	4.1	−9.0	−69.8	−206.5
ΔE(H11)	76.4	75.4	75.9	46.6	92.2	78.8
ΔE(H12)	75.4	78.1	85.8	85.8	91.3	78.6
$\Delta E(H^+)$	−833.1	−825.7	−848.0	−837.5	−1059.7	−1052.3
−PA	−809.1	−814.1	−842.0	−853.8	−710.5	−731.6
ΔZPVE	31.3	32.3	33.2	34.0	31.2	29.5
ϵ	3.4	2.9	0.7	−0.7	−0.2	0.9

[a] All values in kJ mol^{-1}.

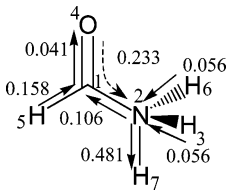

Figure 6. B3LYP/6-31++G**//B3LYP/6-31G** QTAIM computed σ (continuous arrows) and π (points arrow) electron interatomic transfers for N-protonation of formamide. All values are in au.

hand, the QTAIM $E(\Omega)$ values indicate that the proton is always more stabilized in the N-protonated species than in the O-protonated species (Table 3). The smaller PAs in N-protonation are due to the important destabilization of the nitrogen bonded to the proton (489.3 and 517.9 kJ mol^{-1}), whereas the energy of the oxygen bonded to the proton does not differ from that presented in the neutral form by more than 36.5 kJ mol^{-1}. The variation of atomic energies is related, once again, to the transfer of electron population. Thus, N-protonation is destabilized with regard to O-protonation because of the lower electronegativity of nitrogen, which allows the transfer of more charge to the proton from a better attractor (0.49 au from nitrogen instead of 0.34 au from oxygen).

The QTAIM study of the neutral, N-protonated, and O-protonated forms of formamide provide a model to compare with some detail the electron charge reorganization involved in O- and N-protonations. On one hand, the O-protonation (Figure 3) involves the transfer of σ-electron charge from oxygen to proton. At the same time, the protonated oxygen recuperates the charge in two ways: a certain amount of σ-electron population from its attached carbon (that also receives electron charge from its bonded hydrogen) and some π-charge, mainly taken from the nitrogen through the mechanism shown in Figure 4. Part of this π charge is recuperated by the nitrogen with σ transfers from attached hydrogens. On the other hand, the N-protonation (Figure 6) takes place with a σ-electron transfer from nitrogen to the hydrogen. This charge is recuperated through a σ-electron transfer from the hydrogens and with a π-electron transfer, basically provided by the oxygen. The largest difference between both protonations appears as an important σ-transfer observed from nitrogen to oxygen (opposite to the π transfer) in the N-protonation, whereas this transfer is not present in O-protonation.

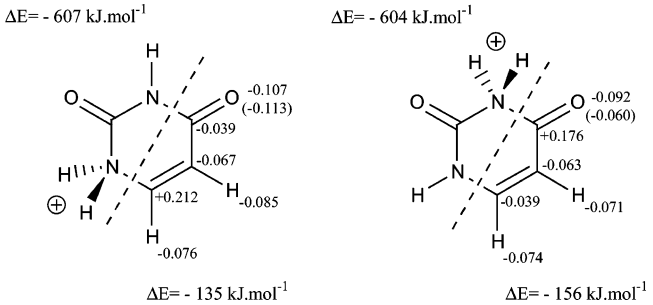

Figure 7. Variation of the atomic energy experienced by C_3H_2O and $[NH_2\text{-}CO\text{-}NH]^+$ fragments of uracil in the N-protonation processes. The variations of atomic electron populations within the C_3H_2O fragment (in au) are also shown. ΔN^{π}(O10) in parentheses.

The protonation of uracil at N3 is favored over that at N1 by more than 21 kJ mol^{-1}. It should to be noticed that this trend is not followed by N-protonations of more simple compounds. Thus, the B3LYP/6-31++G** PAs computed for N-formylformamide and N-vinylformamide are, respectively, 687 and 776 kJ mol^{-1}, and the PAs of formamide and vinylamine computed at the same level are, respectively, 778 and 894 kJ mol^{-1}. So, no model compounds can be employed, and we have to analyze directly the differences of both protonations in uracil.

The variations of atomic energies due to both protonations can be grouped considering the uracil molecule split into the two regions shown in Figure 7. Although the $[H_2N{-}CO{-}NH]^+$ region displays the largest variation of energy, its behavior is practically the same in both protonations. On the contrary, the C_3H_2O region experiences energy variations that are significant different in both protonations. This difference is practically that observed between both N-protonated species. Looking at the variation of atomic energies in this region (Table 3), we observe that the carbonyl group (C4═O10) becomes very stabilized by protonation at N3, whereas the protonation at N1 stabilizes preferentially the C5═C6 area. Both facts can be easily explained because of the position of the large positive charge in each case. As the electronic population of the C4═O10 region is larger than that of the C5═C6 one, the first relative stabilization exceeds the second one, and protonation at N3 results is favored.

Both N-protonations are accompanied by the same electron charge transfer from the C_3H_2O region to the $[H_2N{-}CO{-}NH]^+$ one (0.161 au). Nevertheless, the charge reorganization is different in both processes: (i) in the protonation at N1, the electron population grows for C6 and decreases in the remaining atoms, with an important π-electron transfer from O10 (0.113 au); (ii) on the contrary, in the protonation at N3, N(C4) increases (less than C6 in the other process, i.e., 0.173 au vs 0.213 au), and the electron populations of the remaining atoms decrease (also less than in the other process). It has to be mentioned that despite losing electron charge, O10 becomes stabilized in both processes, although the origin of this stabilization is different in every case: repulsions diminish and attractions increase in the N3 protonation, whereas increased attractions exceed increased repulsions for protonation at N1.

Conclusion

The research reported in this work confirms the results presented in part I[1] about the inadequacy of the RM to describe the electronic effects experienced by pyrimidinic bases upon protonation. On the contrary, QTAIM provides simple explanations for the stability sequence of protonated forms of uracil where σ-electron reorganization and electronegativity play a

significant role. Thus, the QTAIM study of neutral and protonated forms of uracil allow us to conclude that

(a) O-protonation is basically favored over the N-protonation because of the lower electron population transferred to the proton from better attractors. Although the proton becomes more stabilized by a larger electron population, this does not compensate the destabilization experienced by the protonated atom, which is the one that transfers the electron population gained by the proton. Thus, the less electronegative the protonated atom, the larger the electron charge transferred to the proton and the lower the stabilization of the protonated form.

(b) The reorganization of electron charge upon protonation is substantially different for the O═C−C═C and O═C−C−X (X = N, O) units. Whereas the former unit allows a more efficient reorganization (with large π transfers and σ transfers extended throughout the whole molecule), the C−X bond acts as a barrier for σ-charge transfers in the latter unit. Thus, protonation at O10 (involved in one O═C−C═C unit and one O═C−C−NHR unit) is favored over protonation at O8 (involved in two O═C−C−NHR units).

(c) The stability sequence of N-protonated forms can be rationalized in terms of the closer position of the proton, when attached to N3, to regions of larger electron population (two carbonyl groups) than when attached to N1 (one carbonyl group and a double bond).

Acknowledgment. We are indebted to Prof. R. F. W. Bader for providing us with a copy of the AIMPAC package of programs. Interesting opinions from Prof. Fall Diop are deeply acknowledged.

References and Notes

(1) González Moa, M. J.; Mosquera, R. A. *J. Phys. Chem. A* **2003**, *107*, 5361.

(2) Bader, R. F. W. *Atoms in Molecules: A Quantum Theory*; Oxford University Press: New York, 1990.

(3) Bader, R. F. W. *Chem. Rev.* **1991**, *91*, 893.

(4) Mandado, M.; Van Alsenoy, C.; Mosquera, R. A. *J. Phys. Chem. A* **2004**, *108*, 7050.

(5) De Proft, F.; Van Alsenoy, C.; Peeters, A.; Langenaeker, W.; Geerlings, P. *J. Comput. Chem.* **2002**, *23*, 1198.

(6) Rousseau, B.; Peeters, A.; Van Alsenoy, C. *Chem. Phys. Lett.* **2000**, *324*, 189.

(7) Hirshfeld, F. L. *Theor. Chim. Acta* **1977**, *44*, 129.

(8) Wiberg, K. B.; Laidig, K. E. *J. Am. Chem. Soc.* **1987**, *109*, 5935.

(9) Wiberg, K. B.; Breneman, C. M. *J. Am. Chem. Soc.* **1992**, *114*, 831.

(10) Laidig, K. E.; Cameron, L. M. *J. Am. Chem. Soc.* **1996**, *118*, 1737.

(11) Vila, A.; Mosquera, R. A. *J. Phys. Chem. A* **2000**, *104*, 12006.

(12) Vila, A.; Mosquera, R. A. *Chem. Phys. Lett.* **2000**, *332*, 474.

(13) Vila, A.; Mosquera, R. A. *Tetrahedron* **2001**, *57*, 9415.

(14) Frisch, M. J.; Trucks, G. W.; Schlegel, H. B.; Scuseria, G. E.; Robb, M. A.; Cheeseman, J. R.; Zakrzewski, V. G.; Montgomery, J. A., Jr.; Stratmann, R. E.; Burant, J. C.; Dapprich, S.; Millam, J. M.; Daniels, A. D.; Kudin, K. N.; Strain, M. C.; Farkas, O.; Tomasi, J.; Barone, V.; Cossi, M.; Cammi, R.; Mennucci, B.; Pomelli, C.; Adamo, C.; Clifford, S.; Ochterski, J.; Petersson, G. A.; Ayala, P. Y.; Cui, Q.; Morokuma, K.; Malick, D. K.; Rabuck, A. D.; Raghavachari, K.; Foresman, J. B.; Cioslowski, J.; Ortiz, J. V.; Baboul, A. G.; Stefanov, B. B.; Liu, G.; Liashenko, A.; Piskorz, P.; Komaromi, I.; Gomperts, R.; Martin, R. L.; Fox, D. J.; Keith, T.; Al-Laham, M. A.; Peng, C. Y.; Nanayakkara, A.; Gonzalez, C.; Challacombe, M.; Gill, P. M. W.; Johnson, B.; Chen, W.; Wong, M. W.; Andres, J. L.; Gonzalez, C.; Head-Gordon, M.; Replogle, E. S.; Pople, J. A. *Gaussian 98*, Revision A.7; Gaussian, Inc.: Pittsburgh, PA, 1998.

(15) Bader, R. F. W. et al. *AIMPAC: A suite of programs for the AIM theory*; McMaster University: Hamilton, Ontario, Canada.

(16) Graña, A. M.; Mosquera, R. A. *Recent Res. Devel. Chem. Phys.* **2001**, *2*, 23.

(17) Haaland, A.; Helgaker, T. U.; Ruud, K., Shorokhov, D. J. *J. Chem. Educ.* **2000**, *77*, 1076.

(18) Jensen, F. *Introduction To Computational Chemistry*; John Wiley and Sons: New York, 1999.

(19) Guerra, C. F.; Handgraaf, J.-W.; Baerends, E. J.; Bickelhaupt, F. *J. Comput. Chem.* **2003**, *25*, 189.

(20) Bader, R. F. W.; Matta, C. F. *J. Phys. Chem. A* **2004**, *108*, 8385.

(21) Flükiger, F. Ph.D. Thesis, University of Genève, 1992.

(22) Portmann, S.; Lüthi, H. P. *CHIMIA* **2000**, *54*, 7.